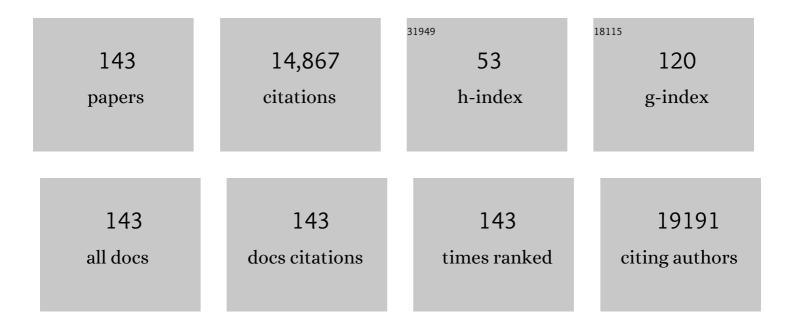
## Niall McEvoy

List of Publications by Year in descending order

Source: https://exaly.com/author-pdf/454964/publications.pdf Version: 2024-02-01



#	Article	IF	CITATIONS
1	Scalable production of large quantities of defect-free few-layer graphene by shear exfoliation in liquids. Nature Materials, 2014, 13, 624-630.	13.3	1,958
2	Oxidation Stability of Colloidal Two-Dimensional Titanium Carbides (MXenes). Chemistry of Materials, 2017, 29, 4848-4856.	3.2	1,120
3	Liquid exfoliation of solvent-stabilized few-layer black phosphorus for applications beyond electronics. Nature Communications, 2015, 6, 8563.	5.8	921
4	Transparent, Flexible, and Conductive 2D Titanium Carbide (MXene) Films with High Volumetric Capacitance. Advanced Materials, 2017, 29, 1702678.	11.1	756
5	Additive-free MXene inks and direct printing of micro-supercapacitors. Nature Communications, 2019, 10, 1795.	5.8	649
6	Highâ€₽erformance Sensors Based on Molybdenum Disulfide Thin Films. Advanced Materials, 2013, 25, 6699-6702.	11.1	435
7	Edge and confinement effects allow in situ measurement of size and thickness of liquid-exfoliated nanosheets. Nature Communications, 2014, 5, 4576.	5.8	432
8	Stamping of Flexible, Coplanar Microâ€&upercapacitors Using MXene Inks. Advanced Functional Materials, 2018, 28, 1705506.	7.8	427
9	A Commercial Conducting Polymer as Both Binder and Conductive Additive for Silicon Nanoparticle-Based Lithium-Ion Battery Negative Electrodes. ACS Nano, 2016, 10, 3702-3713.	7.3	394
10	Direct Observation of Degenerate Two-Photon Absorption and Its Saturation in WS <sub>2</sub> and MoS <sub>2</sub> Monolayer and Few-Layer Films. ACS Nano, 2015, 9, 7142-7150.	7.3	322
11	High-Performance Hybrid Electronic Devices from Layered PtSe <sub>2</sub> Films Grown at Low Temperature. ACS Nano, 2016, 10, 9550-9558.	7.3	310
12	Basal-Plane Functionalization of Chemically Exfoliated Molybdenum Disulfide by Diazonium Salts. ACS Nano, 2015, 9, 6018-6030.	7.3	293
13	High areal capacity battery electrodes enabled by segregated nanotube networks. Nature Energy, 2019, 4, 560-567.	19.8	281
14	Production of Molybdenum Trioxide Nanosheets by Liquid Exfoliation and Their Application in High-Performance Supercapacitors. Chemistry of Materials, 2014, 26, 1751-1763.	3.2	266
15	Investigation of the optical properties of MoS <sub>2</sub> thin films using spectroscopic ellipsometry. Applied Physics Letters, 2014, 104, 103114.	1.5	255
16	High capacity silicon anodes enabled by MXene viscous aqueous ink. Nature Communications, 2019, 10, 849.	5.8	253
17	Electrochemical ascorbic acid sensor based on DMF-exfoliated graphene. Journal of Materials Chemistry, 2010, 20, 7864.	6.7	224
18	In Situ Formed Protective Barrier Enabled by Sulfur@Titanium Carbide (MXene) Ink for Achieving High apacity, Long Lifetime Liâ€\$ Batteries. Advanced Science, 2018, 5, 1800502.	5.6	210

#	Article	IF	CITATIONS
19	Plasma-assisted simultaneous reduction and nitrogen doping of graphene oxide nanosheets. Journal of Materials Chemistry A, 2013, 1, 4431.	5.2	198
20	Preparation of Gallium Sulfide Nanosheets by Liquid Exfoliation and Their Application As Hydrogen Evolution Catalysts. Chemistry of Materials, 2015, 27, 3483-3493.	3.2	195
21	A Robust, Freestanding MXene‣ulfur Conductive Paper for Longâ€Lifetime Li–S Batteries. Advanced Functional Materials, 2019, 29, 1901907.	7.8	195
22	Raman characterization of platinum diselenide thin films. 2D Materials, 2016, 3, 021004.	2.0	172
23	Chemically Modulated Graphene Diodes. Nano Letters, 2013, 13, 2182-2188.	4.5	156
24	Plasma assisted synthesis of WS2 for gas sensing applications. Chemical Physics Letters, 2014, 615, 6-10.	1.2	150
25	Controlled synthesis of transition metal dichalcogenide thin films for electronic applications. Applied Surface Science, 2014, 297, 139-146.	3.1	144
26	Wide Spectral Photoresponse of Layered Platinum Diselenide-Based Photodiodes. Nano Letters, 2018, 18, 1794-1800.	4.5	140
27	Comparison of liquid exfoliated transition metal dichalcogenides reveals MoSe <sub>2</sub> to be the most effective hydrogen evolution catalyst. Nanoscale, 2016, 8, 5737-5749.	2.8	127
28	Highly Sensitive Electromechanical Piezoresistive Pressure Sensors Based on Large-Area Layered PtSe <sub>2</sub> Films. Nano Letters, 2018, 18, 3738-3745.	4.5	125
29	Liquid exfoliation of interlayer spacing-tunable 2D vanadium oxide nanosheets: High capacity and rate handling Li-ion battery cathodes. Nano Energy, 2017, 39, 151-161.	8.2	123
30	Synthesis and analysis of thin conducting pyrolytic carbon films. Carbon, 2012, 50, 1216-1226.	5.4	116
31	Thickness Dependence and Percolation Scaling of Hydrogen Production Rate in MoS <sub>2</sub> Nanosheet and Nanosheet–Carbon Nanotube Composite Catalytic Electrodes. ACS Nano, 2016, 10, 672-683.	7.3	116
32	Mapping of Low-Frequency Raman Modes in CVD-Grown Transition Metal Dichalcogenides: Layer Number, Stacking Orientation and Resonant Effects. Scientific Reports, 2016, 6, 19476.	1.6	111
33	A WSe <sub>2</sub> vertical field emission transistor. Nanoscale, 2019, 11, 1538-1548.	2.8	100
34	MoS <sub>2</sub> Memtransistors Fabricated by Localized Helium Ion Beam Irradiation. ACS Nano, 2019, 13, 14262-14273.	7.3	99
35	Simultaneous electrochemical determination of dopamine and paracetamol based on thin pyrolytic carbon films. Analytical Methods, 2012, 4, 2048.	1.3	95
36	The effect of downstream plasma treatments on graphene surfaces. Carbon, 2012, 50, 395-403.	5.4	95

#	Article	IF	CITATIONS
37	Effect of Percolation on the Capacitance of Supercapacitor Electrodes Prepared from Composites of Manganese Dioxide Nanoplatelets and Carbon Nanotubes. ACS Nano, 2014, 8, 9567-9579.	7.3	89
38	Nitrogen-doped reduced graphene oxide electrodes for electrochemical supercapacitors. Physical Chemistry Chemical Physics, 2014, 16, 2280.	1.3	87
39	Dispersion of nonlinear refractive index in layered WS_2 and WSe_2 semiconductor films induced by two-photon absorption. Optics Letters, 2016, 41, 3936.	1.7	86
40	Characterization of graphene-silicon Schottky barrier diodes using impedance spectroscopy. Applied Physics Letters, 2013, 103, 193106.	1.5	82
41	Heterojunction Hybrid Devices from Vapor Phase Grown MoS2. Scientific Reports, 2014, 4, 5458.	1.6	80
42	Saturation of Two-Photon Absorption in Layered Transition Metal Dichalcogenides: Experiment and Theory. ACS Photonics, 2018, 5, 1558-1565.	3.2	79
43	Functionalisation of graphene surfaces with downstream plasma treatments. Carbon, 2013, 54, 283-290.	5.4	77
44	Large variations in both dark- and photoconductivity in nanosheet networks as nanomaterial is varied from MoS <sub>2</sub> to WTe <sub>2</sub> . Nanoscale, 2015, 7, 198-208.	2.8	76
45	Percolation scaling in composites of exfoliated MoS2 filled with nanotubes and graphene. Nanoscale, 2012, 4, 6260.	2.8	75
46	Electrical devices from top-down structured platinum diselenide films. Npj 2D Materials and Applications, 2018, 2, .	3.9	74
47	Transition Metal Dichalcogenide Growth via Close Proximity Precursor Supply. Scientific Reports, 2014, 4, 7374.	1.6	72
48	Production of Ni(OH) <sub>2</sub> nanosheets by liquid phase exfoliation: from optical properties to electrochemical applications. Journal of Materials Chemistry A, 2016, 4, 11046-11059.	5.2	71
49	Enabling Flexible Heterostructures for Liâ€ion Battery Anodes Based on Nanotube and Liquidâ€Phase Exfoliated 2D Gallium Chalcogenide Nanosheet Colloidal Solutions. Small, 2017, 13, 1701677.	5.2	71
50	Quantum confinement-induced semimetal-to-semiconductor evolution in large-area ultra-thin PtSe2 films grown at 400 °C. Npj 2D Materials and Applications, 2019, 3, .	3.9	69
51	Exfoliation of 2D materials by high shear mixing. 2D Materials, 2019, 6, 015008.	2.0	67
52	Nonlinear Optical Signatures of the Transition from Semiconductor to Semimetal in PtSe <sub>2</sub> . Laser and Photonics Reviews, 2019, 13, 1900052.	4.4	64
53	Ultrafast Carrier Dynamics and Bandgap Renormalization in Layered PtSe <sub>2</sub> . Small, 2019, 15, e1902728.	5.2	60
54	Environmental Effects on the Electrical Characteristics of Back-Gated WSe2 Field-Effect Transistors. Nanomaterials, 2018, 8, 901.	1.9	58

#	Article	IF	CITATIONS
55	Insights into Multilevel Resistive Switching in Monolayer MoS <sub>2</sub> . ACS Applied Materials & Interfaces, 2020, 12, 6022-6029.	4.0	54
56	Coexistence of Negative and Positive Photoconductivity in Few‣ayer PtSe <sub>2</sub> Fieldâ€Effect Transistors. Advanced Functional Materials, 2021, 31, 2105722.	7.8	53
57	Twoâ€Photon Absorption in Monolayer MXenes. Advanced Optical Materials, 2020, 8, 1902021.	3.6	50
58	Molybdenum disulfide/pyrolytic carbon hybrid electrodes for scalable hydrogen evolution. Nanoscale, 2014, 6, 8185.	2.8	48
59	Defect sizing, separation, and substrate effects in ion-irradiated monolayer two-dimensional materials. Physical Review B, 2018, 98, .	1.1	46
60	Pulsed laser deposition of nanoparticle films of Au. Applied Surface Science, 2007, 254, 1303-1306.	3.1	44
61	Layered PtSe <sub>2</sub> for Sensing, Photonic, and (Optoâ€)Electronic Applications. Advanced Materials, 2021, 33, e2004070.	11.1	44
62	Electroanalytical Sensing Properties of Pristine and Functionalized Multilayer Graphene. Chemistry of Materials, 2014, 26, 1807-1812.	3.2	43
63	Optical Imaging and Characterization of Graphene and Other 2D Materials Using Quantitative Phase Microscopy. ACS Photonics, 2017, 4, 3130-3139.	3.2	43
64	Gas phase controlled deposition of high quality large-area graphene films. Chemical Communications, 2010, 46, 1422.	2.2	42
65	Perforating Freestanding Molybdenum Disulfide Monolayers with Highly Charged Ions. Journal of Physical Chemistry Letters, 2019, 10, 904-910.	2.1	42
66	Surface-State Assisted Carrier Recombination and Optical Nonlinearities in Bulk to 2D Nonlayered PtS. ACS Nano, 2019, 13, 13390-13402.	7.3	37
67	Investigations of vapour-phase deposited transition metal dichalcogenide films for future electronic applications. Solid-State Electronics, 2016, 125, 39-51.	0.8	36
68	Extra lithium-ion storage capacity enabled by liquid-phase exfoliated indium selenide nanosheets conductive network. Energy and Environmental Science, 2020, 13, 2124-2133.	15.6	35
69	A New 2H-2H′/1T Cophase in Polycrystalline MoS <sub>2</sub> and MoSe <sub>2</sub> Thin Films. ACS Applied Materials & Interfaces, 2016, 8, 31442-31448.	4.0	33
70	Wafer-Scale Fabrication of Recessed-Channel PtSe <sub>2</sub> MOSFETs With Low Contact Resistance and Improved Gate Control. IEEE Transactions on Electron Devices, 2018, 65, 4102-4108.	1.6	33
71	PtSe <sub>2</sub> grown directly on polymer foil for use as a robust piezoresistive sensor. 2D Materials, 2019, 6, 045029.	2.0	33
72	Organic Electrochemical Transistors (OECTs) Toward Flexible and Wearable Bioelectronics. Molecules, 2020, 25, 5288.	1.7	32

#	Article	IF	CITATIONS
73	CVD growth and processing of graphene for electronic applications. Physica Status Solidi (B): Basic Research, 2011, 248, 2604-2608.	0.7	31
74	Grain boundary-mediated nanopores in molybdenum disulfide grown by chemical vapor deposition. Nanoscale, 2017, 9, 1591-1598.	2.8	31
75	Growth of 1T′ MoTe <sub>2</sub> by Thermally Assisted Conversion of Electrodeposited Tellurium Films. ACS Applied Energy Materials, 2019, 2, 521-530.	2.5	30
76	Helium ion microscope generated nitrogen-vacancy centres in type Ib diamond. Applied Physics Letters, 2014, 104, .	1.5	29
77	Low wavenumber Raman spectroscopy of highly crystalline MoSe <sub>2</sub> grown by chemical vapor deposition. Physica Status Solidi (B): Basic Research, 2015, 252, 2385-2389.	0.7	29
78	Imaging and identification of point defects in PtTe2. Npj 2D Materials and Applications, 2021, 5, .	3.9	29
79	Raman Spectroscopy of Suspended MoS <sub>2</sub> . Physica Status Solidi (B): Basic Research, 2017, 254, 1700218.	0.7	26
80	Optimized single-layer MoS <sub>2</sub> field-effect transistors by non-covalent functionalisation. Nanoscale, 2018, 10, 17557-17566.	2.8	26
81	Thin film pyrolytic carbon electrodes: A new class of carbon electrode for electroanalytical sensing applications. Electrochemistry Communications, 2010, 12, 1034-1036.	2.3	25
82	Investigation of the Interfaces in Schottky Diodes Using Equivalent Circuit Models. ACS Applied Materials & Interfaces, 2013, 5, 6951-6958.	4.0	25
83	Effects of Excitonic Resonance on Second and Third Order Nonlinear Scattering from Few-Layer MoS <sub>2</sub> . ACS Photonics, 2018, 5, 1235-1240.	3.2	25
84	lsotropic conduction and negative photoconduction in ultrathin PtSe2 films. Applied Physics Letters, 2020, 117, 193102.	1.5	25
85	Low-temperature synthesis and electrocatalytic application of large-area PtTe <sub>2</sub> thin films. Nanotechnology, 2020, 31, 375601.	1.3	23
86	Production of monolayer-rich gold-decorated 2H–WS2 nanosheets by defect engineering. Npj 2D Materials and Applications, 2017, 1, .	3.9	22
87	Atomic-Scale Carving of Nanopores into a van der Waals Heterostructure with Slow Highly Charged Ions. ACS Nano, 2020, 14, 10536-10543.	7.3	22
88	Spectroscopic thickness and quality metrics for PtSe <sub>2</sub> layers produced by top-down and bottom-up techniques. 2D Materials, 2020, 7, 045027.	2.0	21
89	Dependence of Photocurrent Enhancements in Quantum Dot (QD) ensitized MoS <sub>2</sub> Devices on MoS <sub>2</sub> Film Properties. Advanced Functional Materials, 2018, 28, 1706149.	7.8	20
90	Calibration of Nonstationary Gas Sensors Based on Two-Dimensional Materials. ACS Omega, 2020, 5, 5959-5963.	1.6	20

#	Article	IF	CITATIONS
91	Rapid high-resolution U–Pb LA-Q-ICPMS age mapping of zircon. Journal of Analytical Atomic Spectrometry, 2017, 32, 262-276.	1.6	18
92	Synthesis and characterisation of thin-film platinum disulfide and platinum sulfide. Nanoscale, 2021, 13, 7403-7411.	2.8	18
93	Inkjet-defined field-effect transistors from chemical vapour deposited graphene. Carbon, 2014, 71, 332-337.	5.4	17
94	Lithium Titanate/Carbon Nanotubes Composites Processed by Ultrasound Irradiation as Anodes for Lithium Ion Batteries. Scientific Reports, 2017, 7, 7614.	1.6	17
95	Fieldâ€Dependent Electrical and Thermal Transport in Polycrystalline WSe <sub>2</sub> . Advanced Materials Interfaces, 2018, 5, 1701161.	1.9	17
96	Influence of Gold Nano-Bipyramid Dimensions on Strong Coupling with Excitons of Monolayer MoS <sub>2</sub> . ACS Applied Materials & Interfaces, 2020, 12, 46406-46415.	4.0	16
97	Few-Layer MoS <sub>2</sub> /a-Si:H Heterojunction Pin-Photodiodes for Extended Infrared Detection. ACS Photonics, 2019, 6, 1372-1378.	3.2	15
98	Vanishing influence of the band gap on the charge exchange of slow highly charged ions in freestanding single-layer <mml:math xmlns:mml="http://www.w3.org/1998/Math/MathML"&gt; <mml:msub> <mml:mi>MoS</mml:mi> <mml:mn>2Physical Review B, 2020, 102, .</mml:mn></mml:msub></mml:math 	:mn> <td>nl:<del>15</del>ub&gt;</td>	nl: <del>15</del> ub>
99	Large-area growth of MoS <sub>2</sub> at temperatures compatible with integrating back-end-of-line functionality. 2D Materials, 2021, 8, 025008.	2.0	14
100	A comparison of catabolic pathways induced in primary macrophages by pristine single walled carbon nanotubes and pristine graphene. RSC Advances, 2016, 6, 65299-65310.	1.7	13
101	Carbon–Silicon Schottky Barrier Diodes. Small, 2012, 8, 1360-1364.	5.2	12
102	Atmospheric pulsed laser deposition and thermal annealing of plasmonic silver nanoparticle films. Nanotechnology, 2017, 28, 445601.	1.3	12
103	Defect-moderated oxidative etching of MoS2. Journal of Applied Physics, 2019, 126, .	1.1	12
104	Long-chain amine-templated synthesis of gallium sulfide and gallium selenide nanotubes. Nanoscale, 2016, 8, 11698-11706.	2.8	11
105	Controlling Defect and Dopant Concentrations in Graphene by Remote Plasma Treatments. Physica Status Solidi (B): Basic Research, 2017, 254, 1700214.	0.7	11
106	Synthesis of tungsten ditelluride thin films and highly crystalline nanobelts from pre-deposited reactants. Tungsten, 2020, 2, 321-334.	2.0	11
107	Effects of Annealing Temperature and Ambient on Metal/PtSe <sub>2</sub> Contact Alloy Formation. ACS Omega, 2019, 4, 17487-17493.	1.6	10
108	Electronic and structural characterisation of polycrystalline platinum disulfide thin films. RSC Advances, 2020, 10, 42001-42007.	1.7	10

#	Article	IF	CITATIONS
109	Dependence of Photocurrent Enhancements in Hybrid Quantum Dot-MoS <sub>2</sub> Devices on Quantum Dot Emission Wavelength. ACS Photonics, 2019, 6, 976-984.	3.2	9
110	Directing the Morphology of Chemical Vapor Depositionâ€Grown MoS <sub>2</sub> on Sapphire by Crystal Plane Selection. Physica Status Solidi (A) Applications and Materials Science, 2020, 217, 2000073.	0.8	9
111	Highly Selective Non ovalent Onâ€Chip Functionalization of Layered Materials. Advanced Electronic Materials, 2021, 7, 2000564.	2.6	9
112	Stepâ€Byâ€6tep Atomic Insights into Structural Reordering from 2D to 3D MoS 2. Advanced Functional Materials, 2021, 31, 2008395.	7.8	9
113	Low Temperature Graphene Growth. ECS Transactions, 2009, 19, 175-181.	0.3	8
114	Microelectronics: Stamping of Flexible, Coplanar Micro‣upercapacitors Using MXene Inks (Adv. Funct.) Tj ETQ	q0.0,0 rgB 7.8	T  Overlock 1
115	Structural and electrical characterisation of PtS from H2S-converted Pt. Applied Materials Today, 2021, 25, 101163.	2.3	7
116	Investigation of carbon-silicon schottky diodes and their use as chemical sensors. , 2013, , .		6
117	Distribution of shallow NV centers in diamond revealed by photoluminescence spectroscopy and nanomachining. Carbon, 2020, 167, 114-121.	5.4	6
118	Nitrogen-doped pyrolytic carbon films as highly electrochemically active electrodes. Physical Chemistry Chemical Physics, 2013, 15, 18688.	1.3	5
119	Suppression of the shear Raman mode in defective bilayer MoS2. Journal of Applied Physics, 2019, 125, .	1.1	5
120	PtSe <sub>2</sub> phototransistors with negative photoconductivity. Journal of Physics: Conference Series, 2021, 1866, 012001.	0.3	5
121	Investigation of 2D transition metal dichalcogenide films for electronic devices. , 2015, , .		4
122	Investigation of carbon–silicon Schottky barrier diodes. Physica Status Solidi (B): Basic Research, 2012, 249, 2553-2557.	0.7	3
123	Remote Plasmaâ€Assisted CVD Growth of Carbon Nanotubes in an Optimised Rapid Thermal Reactor. Chemical Vapor Deposition, 2012, 18, 17-21.	1.4	3
124	Monolayer-enriched production of Au-decorated WS2 Nanosheets via Defect Engineering. MRS Advances, 2018, 3, 2435-2440.	0.5	3
125	Nitrogen as a Suitable Replacement for Argon within Methaneâ€Based Hotâ€Wall Graphene Chemical Vapor Deposition. Physica Status Solidi (B): Basic Research, 2019, 256, 1900240.	0.7	2
126	Multiphoton Absorption and Graphitization in Poly(methyl methacrylate)-Coated Aluminum Nanoantenna Arrays. Journal of Physical Chemistry C, 2020, 124, 8930-8937.	1.5	2

#	Article	IF	CITATIONS
127	Feasibility of graphene–polymer composite membranes for forward osmosis applications. Materials Advances, 0, , .	2.6	2
128	Electrical Conduction and Photoconduction in PtSe2 Ultrathin Films. Materials Proceedings, 2020, 4, .	0.2	2
129	Investigations of vapor phase deposited transition metal dichalcogenide films for future electronic applications. , 2015, , .		1
130	Optimisation of copper catalyst by the addition of chromium for the chemical vapour deposition growth of monolayer graphene. Carbon, 2015, 95, 789-793.	5.4	1
131	Patterning Functionalized Surfaces of 2D Materials by Nanoshaving. Nanomanufacturing and Metrology, 2022, 5, 23-31.	1.5	1
132	Excitonâ€Like and Midâ€Gap Absorption Dynamics of PtS in Resonant and Transparent Regions. Laser and Photonics Reviews, 2022, 16, .	4.4	1
133	Growth of Carbon Nanotubes on Si Substrate Using Fe Catalyst Produced by Pulsed Laser Deposition. Journal of Nanoscience and Nanotechnology, 2008, 8, 5748-5752.	0.9	0
134	Low wavenumber Raman spectroscopy of highly crystalline MoSe2 grown by chemical vapor deposition (Phys. Status Solidi B 11/2015). Physica Status Solidi (B): Basic Research, 2015, 252, .	0.7	0
135	Enhancing the electrical properties of MoS <inf>2</inf> through nonradiative energy transfer. , 2017, ,		0
136	Ex-situ plasma doping of MoS <inf>2</inf> thin films synthesised by thermally assisted conversion process: Simulations and experiment. , 2017, , .		0
137	Nonradiative Energy Transfer and Photocurrent Enhancements in Hybrid Quantum Dot-MoS <inf>2</inf> Devices. , 2018, , .		0
138	Rabi Splitting using Gold Nano-Bipyramids and Monolayer MoS2. , 2021, , .		0
139	Influence of Nanoparticle Dimensions on Rabi Splitting Strength. , 2021, , .		Ο
140	Nonlinear absorption in WS2 and MoS2 mono- and few-layer films. , 2016, , .		0
141	Manipulation of Transition Metal Dichalcogenides: Nanomachining 2D PtSe2 using AFM. , 0, , .		Ο
142	Nonlinear optical properties and ultrafast carrier dynamics in two-dimensional PtSe2 materials. , 2019, , .		0
143	Manipulation of Transition Metal Dichalcogenides: Nanomachining 2D PtSe2 using AFM. , 0, , .		Ο